JOURNAL OF MATERIALS SCIENCE **34** (1999) 4399–4411

Crystal nucleation in P_2O_5-doped lithium disilicate glasses

Y. IQBAL*, W. E. LEE*, D. HOLLAND‡, P. F. JAMES*
*Department of Engineering Materials, University of Sheffield, UK
‡Department of Physics, University of Warwick, UK
E-mail: p.f.james@sheffield.ac.uk

The bulk (volume) crystallisation of $Li_2O{\cdot}2SiO_2$ (LS_2) glasses with additions of 1, 2 and 5 mol % P_2O_5 (G1P, G2P and G5P) was investigated. In the G1P and G2P glasses heated at 454 °C metastable α'- and β'-LS_2 crystal phases formed initially and only stable LS_2 at later stages. In G1P heated at 463 °C transmission electron microscopy (TEM) revealed particles ($\geq$2 μm) of stable LS_2 but also smaller ($<$0.1 μm) crystalline particles which were unstable under the electron beam and could not be identified. Crystalline lithium orthophosphate (Li_3PO_4) was detected by XRD and ^{31}P magic angle spinning nuclear magnetic resonance (MAS-NMR) in both as-quenched and heat treated G5P but not in G1P and G2P. In G5P heated at 476 °C, metastable α'-LS_2 phase initially formed and at later times stable LS_2. In as-quenched G5P, a trace of lithium metasilicate (LS) was observed. Li_3PO_4 crystals were not detected in G5P by TEM but a marked increase in nucleation rate due to P_2O_5 addition was observed. ^{29}Si MAS-NMR revealed amorphous Q^2 (LS) and Q^4 (SiO_2) species in an average Q^3 (LS_2) environment in the as-quenched glasses. Increased P_2O_5 concentration caused a greater degree of amorphous phase separation. ^{31}P MAS-NMR showed amorphous lithium phosphate units in the as-quenched and nucleated G1P and G2P. The presence of crystalline Li_3PO_4 phase in glass G5P suggests that Li_3PO_4 crystals may act as sites for heterogeneous nucleation of stable lithium disilicate. © *1999 Kluwer Academic Publishers*

1. Introduction

The objective of this work was to investigate the effect of small amounts (1–5 mol %) of P_2O_5 on the crystallisation behaviour of $Li_2O{\cdot}2SiO_2$ (LS_2) glass and search for the possible precipitation of Li_3PO_4 nuclei prior to equilibrium crystallisation. Lithium disilicate is a relatively simple composition for nucleation and crystallisation studies [1] and has been examined extensively. Previous research has been summarised by James [2, 3]. P_2O_5 is an effective nucleation agent in the $Li_2O \cdot SiO_2$ system [3, 4]. Pure LS_2 glass has no tendency towards amorphous phase separation [5, 6], but with small additions of P_2O_5 phase separation will occur [7, 8]. The effect of the addition of small percentages of P_2O_5 on the crystallisation behaviour of LS_2 glass has been studied, particularly in glasses containing $\leq$2 mol % P_2O_5 [7–12].

Previous studies [8–11] confirm that small (1–3 mol %) additions of P_2O_5 to LS_2 glass simultaneously induce amorphous phase separation and markedly increase the crystal nucleation rate. However, it is not yet clear [2, 3] whether the observed increase in crystal nucleation rates (I) with P_2O_5 is due to (a) precipitation of Li_3PO_4 or a similar phase [8, 9, 11] with subsequent heterogeneous nucleation of lithium disilicate on Li_3PO_4 crystals or (b) a lowering of the interfacial free energy between the lithium disilicate crystals and surrounding glass as a result of the P_2O_5 addition, leading to enhanced homogeneous nucleation of lithium disilicate [2, 3, 8].

Studies [2, 3, 8–11] indicate that there is no marked direct connection between the presence of amorphous phase separation and the crystal nucleation in these compositions and that crystal nucleation probably occurs in the lithia-rich matrix rather than preferentially at the amorphous droplet interfaces. However, the enhanced phase separation on adding P_2O_5 may be explained [8, 11] by molecular association between Li_2O and P_2O_5 to form lithium phosphate groupings such as Li_3PO_4 in the matrix phase. These groupings might precipitate as submicroscopic crystal nuclei of Li_3PO_4 or a similar phase which would serve to heterogeneously nucleate LS_2 crystals. Supporting this possibility is the close match between the 3.588 Å (111) and 2.406 Å (140) spacings of Li_3PO_4 and 3.59 Å (111) and 2.395 Å (002) spacings of LS_2 [JCPDS card #17-447 & 15-760]. This would permit epitaxial growth. Evidence in favour of such a heterogeneous mechanism is given by Headley and Loehmann [13] who observed precipitates of Li_3PO_4 crystals from a Li_2O-Al_2O_3-SiO_2 based glass after heat treatments in the range 800–1000 °C, and demonstrated epitaxial growth of lithium disilicate on the Li_3PO_4 using TEM. However, the temperatures used were high and no such Li_3PO_4 phase has yet been

observed experimentally in Li_2O-SiO_2 glasses containing $\leq$3 mol % P_2O_5, using XRD or TEM [2–4] for heat treatments in the range of temperatures (450–550 °C) where high crystal nucleation rates occur.

Some additives decrease viscosity and may cause a decrease in the interfacial free energy of the nucleus-glass interface [14]. The observed change in viscosity due to the inclusion of 1 mol % P_2O_5, is too low to account for the effect on the nucleation rate [15], although the reduction in the interfacial energy by addition of P_2O_5 remains a distinct possibility.

Phillips and McMillan [7] explained their electrical resistivity measurement data on the basis that the addition of P_2O_5 increased the extent of two-phase separation and widens the range of phase-separable compositions. They suggested that phase separation favours the formation of small crystals by causing a decrease in the crystal growth rate. McMillan also suggested that the presence of amorphous phase separation in P_2O_5-containing glasses may also indirectly assist nucleation since the SiO_2-rich droplets prevent the coarsening of nuclei [16] causing increased nucleation densities. Such processes would occur if the SiO_2-rich phase hindered the diffusion process necessary to permit coarsening or if P_2O_5 were concentrated at the interface but again no evidence for this has been found [3].

TEM of LS_2 glass with an addition of 3 mol % P_2O_5 revealed glass-in-glass phase separation in the form of 500 Å (diameter) glassy droplets and 1 μm crystals uniformly dispersed at intervals of 2 μm, although Li_3PO_4 was not reported [4].

^{29}Si MAS-NMR of lithium silicate glasses has been mostly performed on as-quenched specimens or on samples nucleated in a limited time-temperature range [17–20]. Good summaries of these studies are given by Kirkpatrick [21], Dupree and Holland [22], Emerson *et al.* [23] and Stebbins *et al.* [24]. MAS-NMR data of Dupree *et al.* [17] showed that the addition of 1 to 5 mol % P_2O_5 to LS_2-glasses increased the polymerisation of the silicate network by effective removal of the modifier (Li^+) cations (supporting the earlier work [8, 11]) and P_2O_5 did not itself participate in the network. MAS-NMR detected only one type of phosphorus site, similar to those in Li_3PO_4. Considering the ratio of alkali to network former [i.e. $(Li_2O)/(SiO_2 + P_2O_5)$] or the ratio of alkali to phosphorus (i.e. Li_2O/P_2O_5) reveals that the former ratio is <1 for 1 to 5 mol % P_2O_5-concentrations. If Li^+ cations are assumed uniformly distributed throughout the network, the association with phosphorus would be much less than that observed [17]. Assuming Li^+ are completely associated with phosphorus for the latter ratio, then only Li_3PO_4 would be observed. Three Li^+ associate with $(PO_4)^{3-}$ units in glass to produce an environment like that in crystalline Li_3PO_4, implying that there is little interaction between them and the silica network. This observation of Li_3PO_4 type units in LS_2 glasses is indirect evidence that Li_3PO_4 nuclei behave as nucleation sites for LS_2.

Most studies are consistent with the observation that P_2O_5 increases nucleation rate, decreases growth rate and induces amorphous phase separation in LS_2 glass. However, the detailed phase transformation sequence has not been fully elucidated. Therefore, a detailed examination of as-quenched and nucleated 1, 2 and 5 mol % P_2O_5-doped LS_2 glasses was carried out in the present study, using XRD, optical microscopy, TEM and MAS-NMR.

Recently, in a study of the early stages of crystallisation of a lithium disilicate glass (without P_2O_5 addition) [25], two metastable crystalline phases, denoted α' and β'-LS_2, precipitated prior to crystallisation of stable lithium disilicate in samples heat treated at 454 °C for 120 to 180 h. These metastable phases (α' could be indexed in terms of a monoclinic symmetry and β' was similar to stable LS_2) probably transformed to stable LS_2 after extended holds at 454 °C. The present study was also carried out to investigate if such metastable phases formed in glasses containing P_2O_5 additions.

2. Experimental

Lithium disilicate (LS_2) glass (G1) and glasses of lithium disilicate composition with additions of 1, 2 and 5 mol % of P_2O_5 (G1P, G2P and G5P) were prepared by melting 100 g batches of standard laboratory reagent grade lithium carbonate, general purpose reagent grade acid washed silica and lithium orthophosphate in a Pt-Rh-crucible at 1350–1470 °C for 5 h in an electric furnace. To avoid violent reaction during melting, the batches were sintered (before melting) for 10 h at 1000 °C in a platinum container. Stirring was carried out with a platinum blade for five hours to ensure homogeneity. The melt was poured onto a steel plate and rapidly quenched (in air) by pressing between steel plates to prevent crystallisation. For MAS-NMR studies, the same G1, G1P, G2P and G5P compositions (Table I) were melted but with 0.05 mol % Fe_2O_3 added to reduce ^{29}Si relaxation time and the resulting compositions were denoted by G1F, G1PF, G2PF and G5PF.

Samples ($\sim 10 \times 10 \times 1.5$ mm^3 pieces) were crystallised by heat treatment in a tube furnace at 454 °C and above for XRD studies. Heat treatment temperatures were maintained constant to within ± 1 °C. Preliminary optical microscopy and TEM of G1P and G2P subjected to nucleation treatments showed that crystals forming

TABLE I Nominal and analysed (by ICPAES) chemical compositions of G1, G1P and G2P glasses; nominal composition for G5P glass

		Nominal		Analysed	
	Oxide	mol %	wt %	mol %	wt %
G1	SiO_2	66.66	80.08	66.09 ± 0.16	79.67 ± 0.2
	Li_2O	33.33	19.91	33.91 ± 0.13	20.33 ± 0.08
G1P	SiO_2	66.00	77.85	66.86 ± 0.17	78.86 ± 0.2
	Li_2O	33.00	19.36	32.21 ± 0.14	18.90 ± 0.08
	P_2O_5	1.00	2.79	0.80 ± 0.007	2.240 ± 0.02
G2P	SiO_2	65.33	75.70	66.24 ± 0.17	76.75 ± 0.2
	Li_2O	32.66	18.82	31.20 ± 0.14	17.98 ± 0.08
	P_2O_5	2.00	5.47	1.91 ± 0.007	5.23 ± 0.02
G5P	SiO_2	63.33	69.68	—	—
	Li_2O	31.66	17.33	—	—
	P_2O_5	5.00	12.99	—	—

at 454 °C were too small and highly electron/ion beam sensitive to be characterised. Therefore, for optical and TEM studies heat treatments were performed at higher temperatures (476 and 550 °C for G1P and G2P respectively) compared to 454 °C used for the P_2O_5-free LS_2 [G1] glass [25]. This produced large (>1 μm) crystals which were observed using optical microscopy. G5P samples also required higher heat treatment temperatures (800 °C) to form ~0.2 μm crystals.

For XRD, the surface crystallised layers of as-quenched and heat treated samples were removed before grinding the remainder to powder and scanning from 10° to 60°, at scanning speeds of 0.25 and 0.125°/min, in a Philips diffractometer (with CuK_α-radiation, $\lambda =$ 0.1541838 nm) at 50 kV and 30 mA. The diffractometer was calibrated with an α-quartz standard sample. Lithium disilicate crystals provided an internal standard for calibration.

Standard TEM specimen preparation techniques were used involving grinding, polishing, dimpling, ion thinning and carbon coating. A JEOL 200CX TEM operating at 200 kV was used to examine the partially crystallised samples. Lithium disilicate or single crystal Si were used as standards for the camera constant (λL) calibration where λ is the electron wavelength and L the camera length. For each crystal at least three selected area diffraction patterns (SADPs) were indexed and interzonal angles calculated with an in-house computer program [26]. To confirm pattern indexing and check for forbidden reflections, the "Diffract" program [27] was used to simulate diffraction patterns. This structure factor based computer package calculates interplanar spacings, d_{hkl}, from the input unit cell parameters, crystal system and atomic co-ordinates.

NMR was carried out using a Bruker MSL 360 spectrometer and Bruker 4 or 7 mm MAS probes. The rotors were Si_3N_4 or ZrO_2 depending on the nucleus being studied. MAS spectra were obtained for ^{29}Si and ^{31}P at spinning speeds of 3–5.5 kHz and 10 kHz respectively to allow separation of the isotropic peaks from the spinning sidebands. ^{29}Si spectra were acquired at a frequency of 71.525 MHz using a pulse length of 2 μs and delays of 1 to 64 s. The ^{31}P spectra were acquired at 145.78 MHz with a pulse length of 3 μs and delay of 1 s. Typically 100 Hz line broadening was applied to the spectra prior to Fourier transformation. The spectra were referenced to tetramethylsilane or 85% H_3PO_4 as appropriate.

3. Results

G1, G1P and G2P glasses were transparent, with no residual batch, visible bubbles, streaks, colours or opalescence as examined by eye. Chemical analysis of G1, G1P and G2P by inductively coupled plasma atomic emission spectroscopy (ICPAES) showed that the nominal and analysed compositions were in close agreement (Table I). Owing to its higher P_2O_5 concentration glass G5P was opalescent due to amorphous phase separation in spite of rapid quenching [17].

3.1. X-ray diffraction

Fig. 1 shows XRD data from G1P heated at 454 °C. After 50 h the trace suggested a completely amorphous sample while peaks due to α'-LS_2 phase [25] emerged after 116 h (Fig. 1a) increasing in intensity up to 212 h (Fig. 1b). β'-LS_2 peaks emerged after 308 h (Fig. 1c). The α'- and β'-LS_2 phases have been previously identified in binary LS_2 glasses at early and intermediate stages of crystallisation at 454 °C [25]. Further increase in heat treatment time caused a continuous decrease in the α'- and β'-LS_2 peak intensities with a subsequent increase in the intensities of stable LS_2 peaks (Fig. 1d), confirming the transformation of the former phases into the latter with time as in the LS_2 glass without P_2O_5 [25].

XRD of G2P heated at 454 °C showed that small peaks due to α'-LS_2 phase appeared over the glassy hump after 47 h (the traces for G2P are not shown), i.e. much earlier than observed for G1P. XRD of G2P subjected to longer holds at 454 °C, revealed decreased

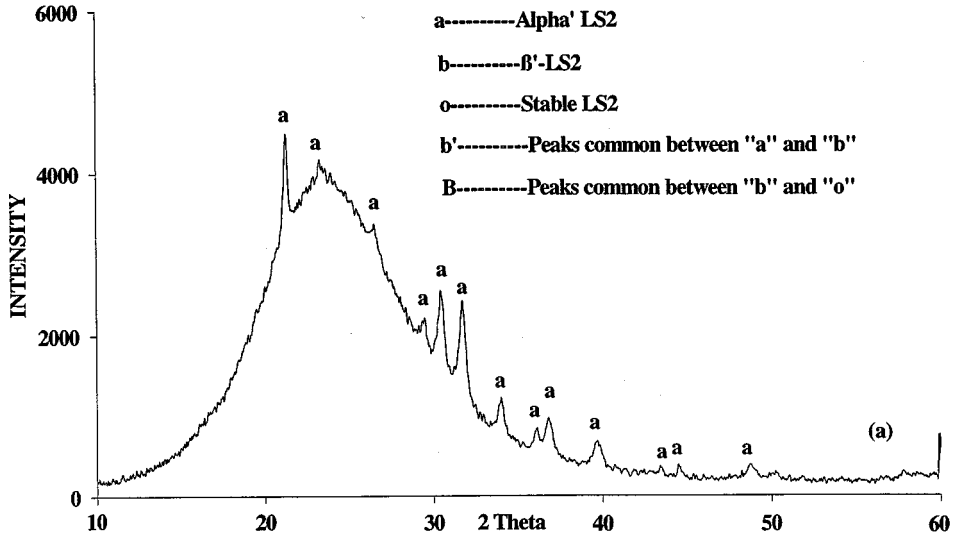

Figure 1 XRD traces of G1P glass ($33Li_2O$-$66SiO_2$-$1P_2O_5$) heat treated at 454 °C for (a) 116 h, (b) 212 h, (c) 308 h and (d) 551 h, showing the presence of α'-, β'- and stable-LS_2 phases at the early, intermediate and later stages of crystallisation respectively. (*Continued*.)

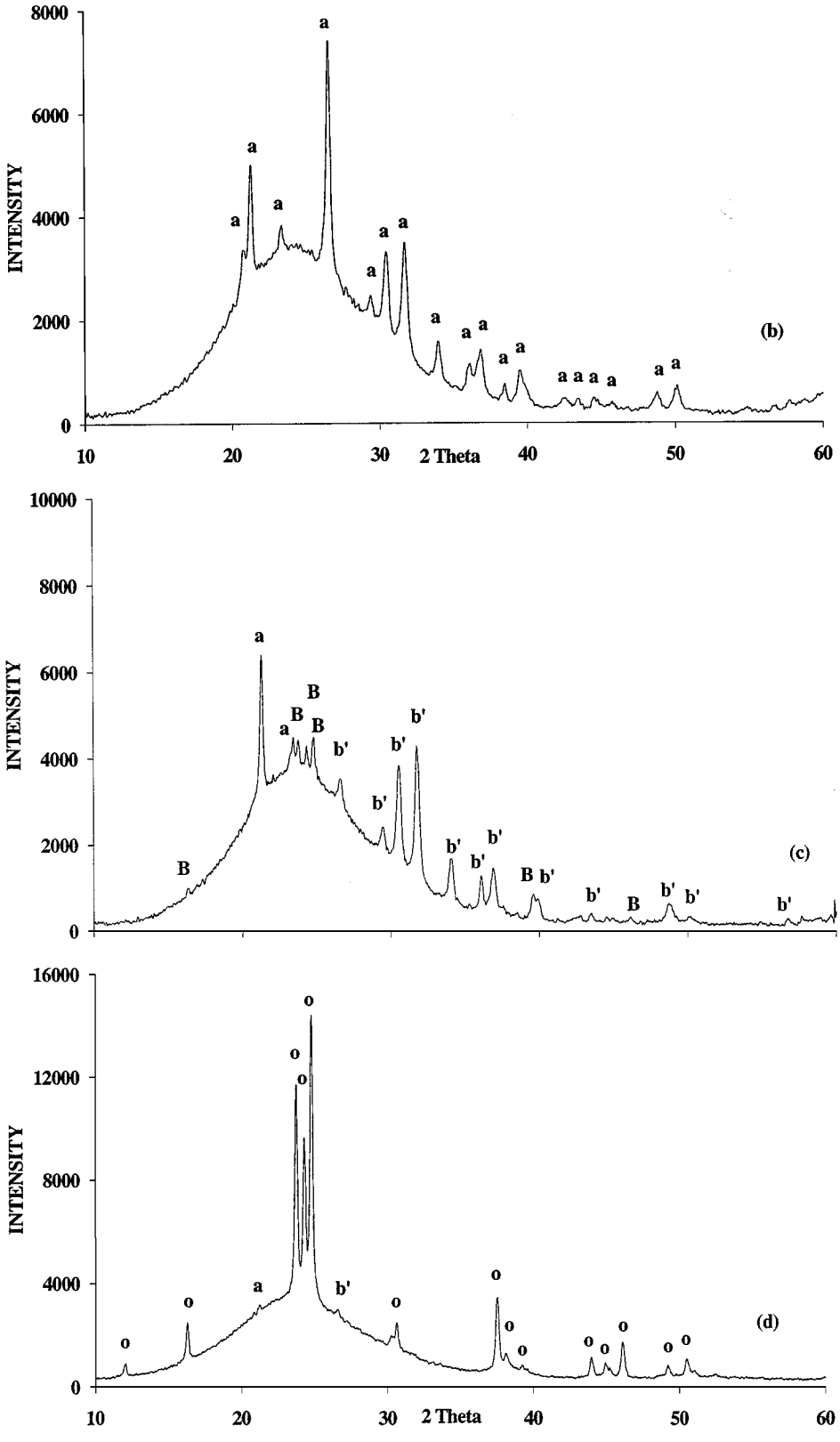

Figure 1 (*Continued*.)

α'-LS_2 peak intensities accompanied by the emergence of peaks due to β'-LS_2. Peaks due to α'- and β'-LS_2 phases disappeared on further holds and stable LS_2 was the only phase present after 551 h at 454 °C, indicating its probable transformation from the metastable intermediates α'- and β'-LS_2. At 476 °C α'-LS_2 was observed after 9 h, and even after 24 h, although with lower peak intensities compared to those of stable LS_2. α'/β'-LS_2 phases disappeared with time and after 214 h at 476 °C only stable LS_2 remained.

Most XRD peaks of as-quenched G5P glass matched JCPDS card #15-760 for Li_3PO_4. The amorphous hump on the XRD trace of the as-quenched G5P glass (Fig. 2a) showed it was mostly (∼95%) amorphous. A small peak at $2\theta \approx 26.86^\circ$ ($d_{hkl} = 3.319$ Å) was comparable with the (111) stable lithium metasilicate (LS)

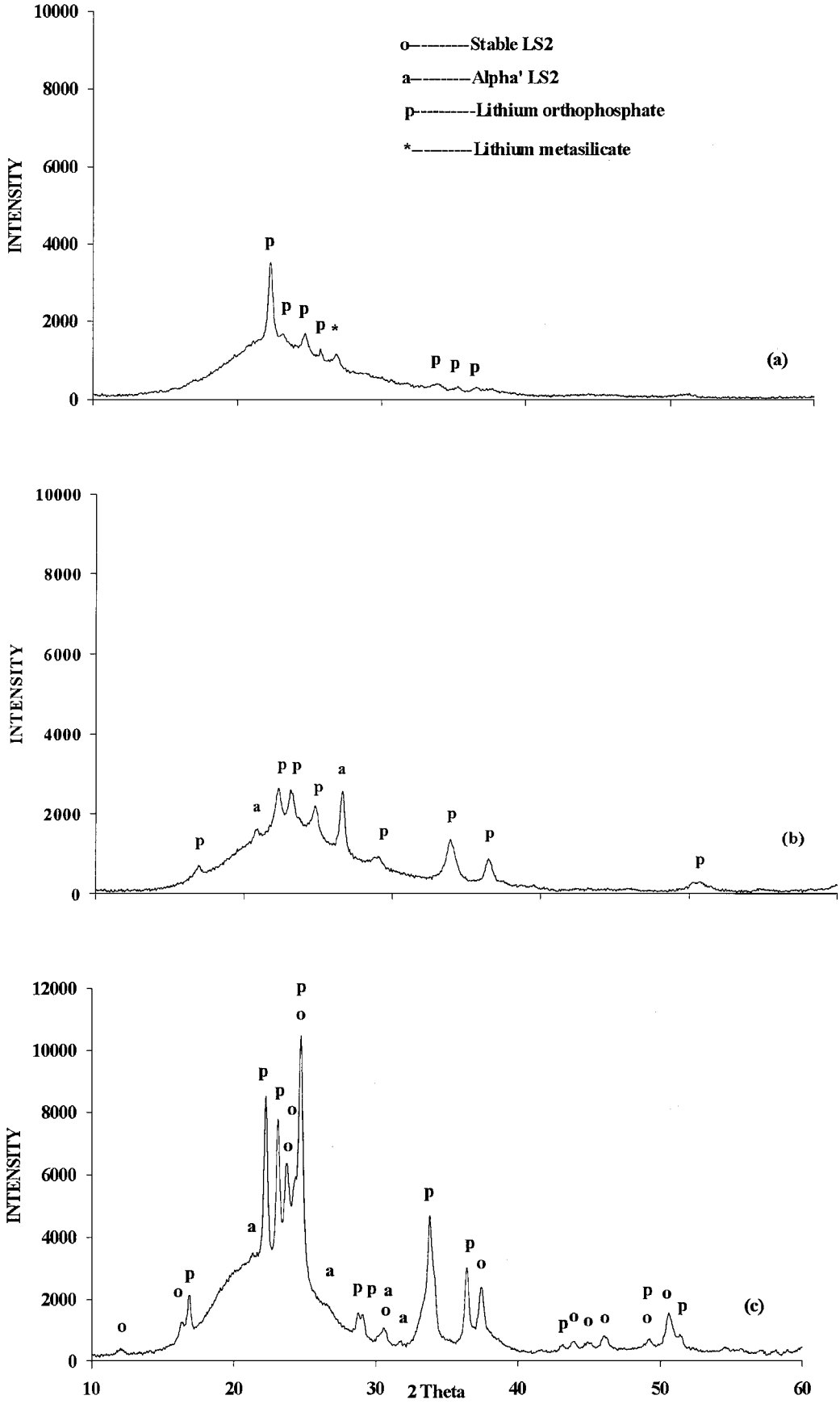

Figure 2 XRD traces of G5P ($31.66Li_2O$-$63.33SiO_2$-$5P_2O_5$) (a) as-quenched glass and heated at 476 °C for (b) 68 h and (c) 214 h, showing the presence of Li_3PO_4, α'-LS_2, LS and stable LS_2 phases at various stages of crystallisation.

peak but other relevant peaks for this compound were missing. No significant crystallisation was observed in G5P heated at 454 °C longer than 300 h so it was heated at 476 °C. Sixty-eight hours hold at 476 °C, caused an increase in the Li_3PO_4 peak intensities and two peaks positioned at $2\theta \approx 20.86°$ ($d_{hkl} = 4.258$ Å) and $26.62°$ ($d_{hkl} = 3.349$ Å) matching the d-spacings 4.26 Å (100) and 3.343 Å (101) for α-quartz (JCPDS card#

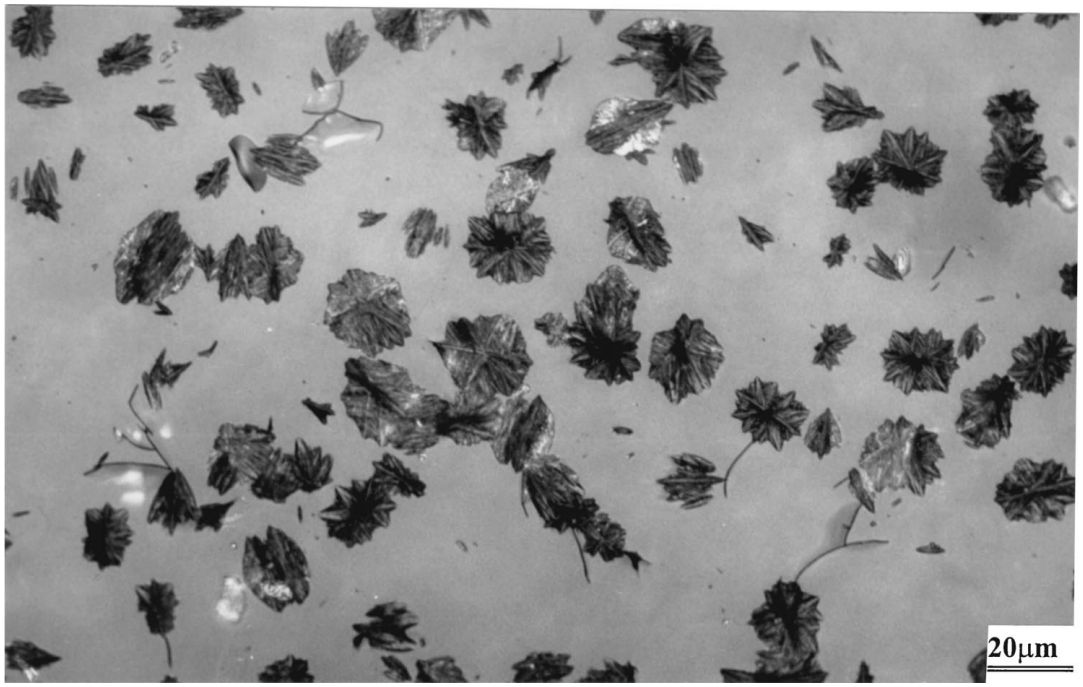

Figure 3a Reflection optical micrograph of G1 heated 122 h at 476 °C. Note the small number density ($\sim 9.5 \times 10^{13}$ m^{-3}) and large size (~ 17 μm) of crystals compared to Fig. 3b.

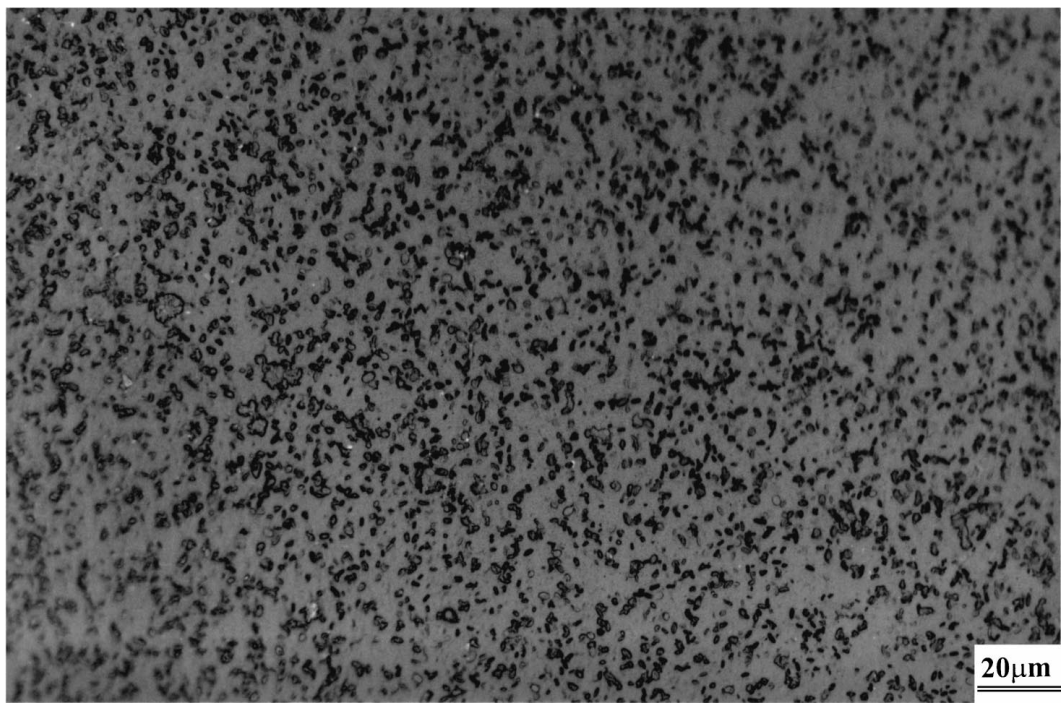

Figure 3b Reflection optical micrograph of G1P heated 122 h at 476 °C, showing a decrease in size (~ 3 μm) and increase in crystal number density ($\sim 5.43 \times 10^{16}$ m^{-3}) due to 1 mol % added P_2O_5.

5-0490) emerged but other relevant α-quartz peaks were not detectable at this volume fraction (Fig. 2b). The latter peak also matches the (111) α'-LS_2 peak [25]. Currently we have no explanation for the 20.86° peak. After 140 h (trace not shown), decreased α'-LS_2 peak intensities were seen due to formation of stable LS_2. In this sample Li_3PO_4 and stable LS_2 phases were both present. After 214 h, peaks due to α'-LS_2 phase had nearly disappeared and Li_3PO_4 and stable LS_2 were the major phases (Fig. 2c) indicating probable transformation of the silicate phases to stable LS_2 with time.

3.2. Optical and transmission electron microscopy

Reflection optical micrographs of G1 and G1P after 122 h at 476 °C are shown in Fig. 3a and b. From these micrographs the number of crystals per unit volume (N_v) were estimated by standard stereological methods [1] and the nucleation rates (I) calculated. Comparing nucleation rates for G1 ($\sim 2.16 \times 10^8$ m^{-3} s^{-1}) and G1P ($\sim 1.23 \times 10^{11}$ m^{-3} s^{-1}) showed that "I" for G1P was ~570 times higher than that for G1. Nucleation rates were also estimated for the G1 and G1P glasses at temperatures close to the corresponding maximum

nucleation temperatures T_{max}, (i.e. 454 and 500 °C respectively see [2]). In this case "*I*" for G1P ($\sim 1.02 \times 10^{13}$ m^{-3} s^{-1}) was ~5000 times higher than that for G1 ($\sim 1.9 \times 10^{9}$ m^{-3} s^{-1}). It should be pointed out that these values are approximate only since no second stage development (growth) treatment was used, and probably significantly underestimate the true values of N_v and I. However, they provide a useful qualitative comparison, and clearly demonstrate the increase of I with P_2O_5 addition, confirming earlier work [2].

TEM of G1P showed that addition of P_2O_5 resulted in a significantly decreased size of the crystals for a given heat treatment time (i.e. a decreased crystal growth rate), an increase in the number density of crystals and decreased stability of the crystals in the electron beam. Fig. 4a–c shows an ellipsoid-shaped crystal ~2 μm in size and a corresponding SADP after 190 h at 463 °C. The SADP was the [001] zone axis of stable LS_2. Apart from the stable LS_2 crystals, even smaller (<0.1 μm) particles were present which rapidly decomposed (or dissolved) on exposure to the electron beam and could not be identified. However, the change in contrast of these particles on tilting the specimen showed them to be crystalline. Ten G1P samples nucleated at 454 and 463 °C for 50–475 h were extensively examined and images and SADPs were recorded at different orientations. All the recordable SADPs were consistent with stable LS_2.

TEM of G2P showed that the addition of 2 mol % P_2O_5 resulted in a further decrease in the size of the crystals for a given heat treatment (i.e. a further decrease in growth rate) and a further increase in their number. Since smaller crystals were more sensitive to electron beam damage, heat treatments at high temperatures (≥520 °C) were required for G2P to produce larger crystals for observation in the TEM. In spite of using the smallest possible condenser aperture and a well-spread beam, it was not possible to control the extensive electron beam damage of these samples. Consequently, single crystals (≤0.2 μm in size) could not be identified. However, general area images and SADPs could be recorded. The interplanar spacings determined from the diffraction rings (recorded for G2P heated 50 h at 520 °C) were 5.45, 3.60, 2.88 and 1.84 Å and were closely comparable (±0.04 Å) with the 5.43 Å (110), 3.59 Å (111), 2.917 Å (200), and 1.831 Å (202) of stable LS_2. XRD of these samples revealed the presence of stable LS_2 only.

Thus an increase in heat treatment temperature caused an increase in the crystal size but no improvement in the stability of samples to electron irradiation. Similarly the crystalline regions (~0.2 μm in size) observed in G5P heated 93 h at 800 °C were identified as stable LS_2 crystals by the corresponding SADPs (e.g. Fig. 5a–c) but no Li_3PO_4 was identified by TEM.

Thus TEM of G1P, G2P and G5P samples gave no evidence of the occurrence of amorphous phase separation or precipitation of Li_3PO_4 (or a similar phase) under the present experimental conditions.

3.3. MAS-NMR

The spectra from ^{29}Si and ^{31}P, for G1PF, G2PF and G5PF are shown in Figs 6 and 7 for different heating times at 454, 476 and 600 °C (depending on the composition). The corresponding chemical shifts are summarised in Tables II and III. ^{29}Si spectra of glasses with no heat treatment are complex (Fig. 6) and contain three distinct species Q^2, Q^3 and Q^4 (the superscript indicates the number of bridging oxygens). The observed distribution would not be predicted by either the statistical (unconstrained) or binary (constrained) models but can be represented by a disproportionated binary distribution in which some non-bridging oxygens have been removed by interaction with phosphate units as described below:

$$2Q^3 \leftrightarrow Q^2 + Q^4 \quad (1)$$

$$6(\text{Si-O}^{-}\,^{+}\text{Li}) + P_2O_5 \leftrightarrow 3(\text{Si-O-Si}) + 2Li_3PO_4 \quad (2a)$$

$$4(\text{Si-O}^{-}\,^{+}\text{Li}) + P_2O_5 \leftrightarrow 2(\text{Si-O-Si}) + Li_4P_2O_7 \quad (2b)$$

Knowing the distribution of phosphate species (see below), the quantities of non-bridging oxygens removed and the effect of the Q distribution can be calculated. The spectra were fitted to a combination of isotropic peaks and spinning sidebands arising from different structural species. An example of such a fit is shown in Fig. 8 for ^{29}Si in G2PF heated 146 h at 454 °C. The percentages of each structural species are plotted versus time in Fig. 9 for the ^{29}Si and ^{31}P in G2PF. This shows that the relative amount of each Q type remains constant for the first few hours of heat treatment, after which, although the quantities of Q^4 and Q^2 are scarcely changed, the amorphous Q^3 is replaced by crystalline Q^3 (denoted by Q^3-X) and some crystalline Q^2-X is also formed. The rate of formation of Q^3-X is rapid at first but then decreases until the amount of Q^3-X is almost constant. Thus transformation is not completed at this temperature over the period used. Complete crystallisation of the glass is achieved after 6 h at 600 °C. Similar

TABLE II ^{29}Si chemical shifts ($\delta \pm 0.5$ ppm) for the as-quenched and heat treated G1PF, G2PF and G5PF samples

Sample	Temperature (°C)	Time (h)	Q^2	Q^3	Q^4
G1PF	Nil	Nil		−90.6	
”	454	93		−90.4	−108
”	”	228		−90.5	−109.5
”	”	408		−92.6	
”	”	500		−92.4	
”	”	Nil		−90.5	
”	”	214	−75.3	−92.7	−110.1
”	600	6		−92.6	
G5PF	476	68	−75.4	−92.6	−110.9

TABLE III ^{31}P chemical shifts ($\delta \pm 0.5$ ppm) for G1PF and G2PF samples after various holds at 454 °C

Sample	Time (h)	δ_1	δ_2	δ_3	δ_4
G1PF	Nil	10.6	0.2		
”	282	10.6	0.2		
”	500	10.6	0.2	−15.9	−26.3
G2PF	336	11.3	1.5		

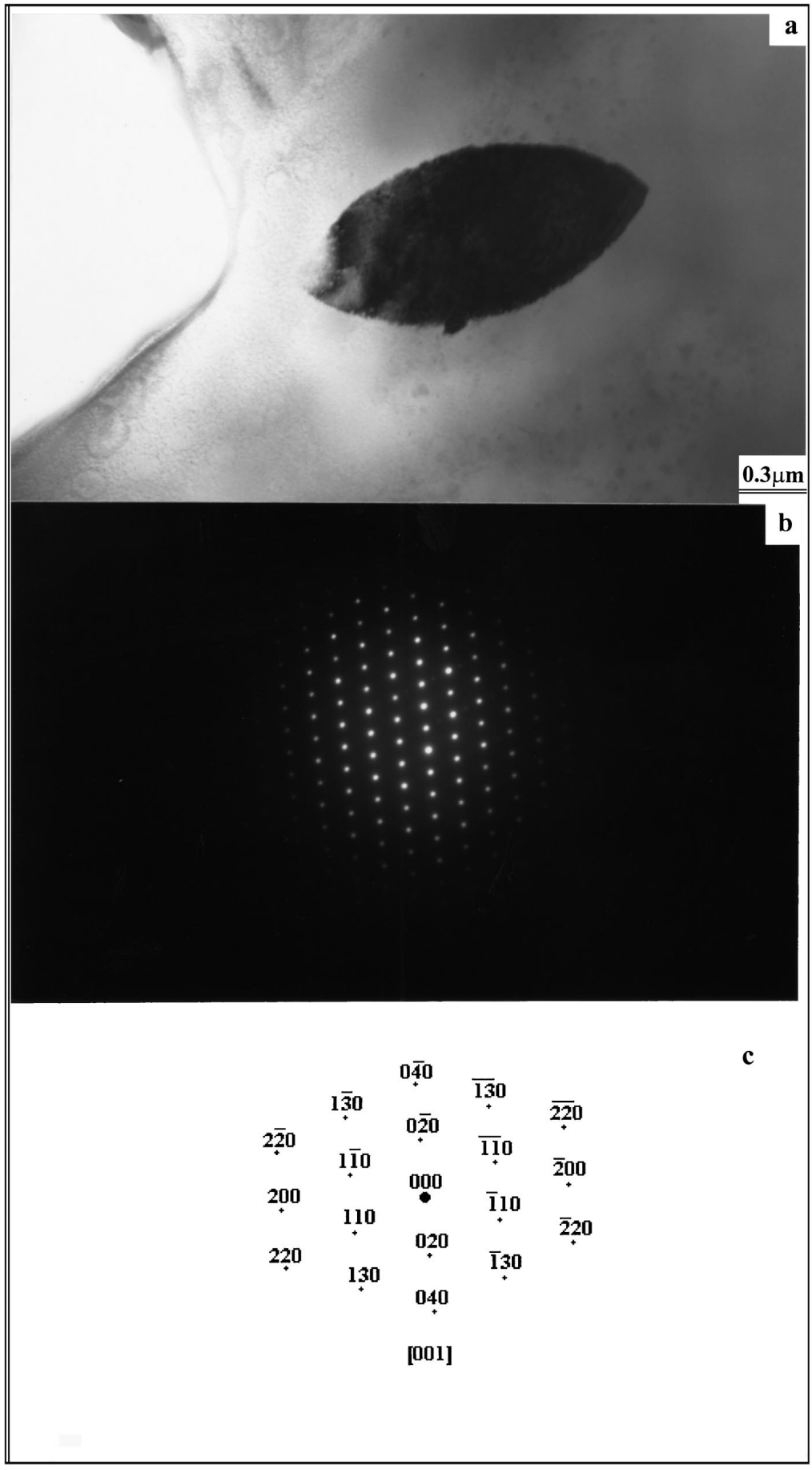

Figure 4 (a) BF TEM image, (b) a corresponding SADP solved in (c); a crystal observed in G1P after 190 h hold at 463 °C. The SADP was indexed as [001] for stable LS_2.

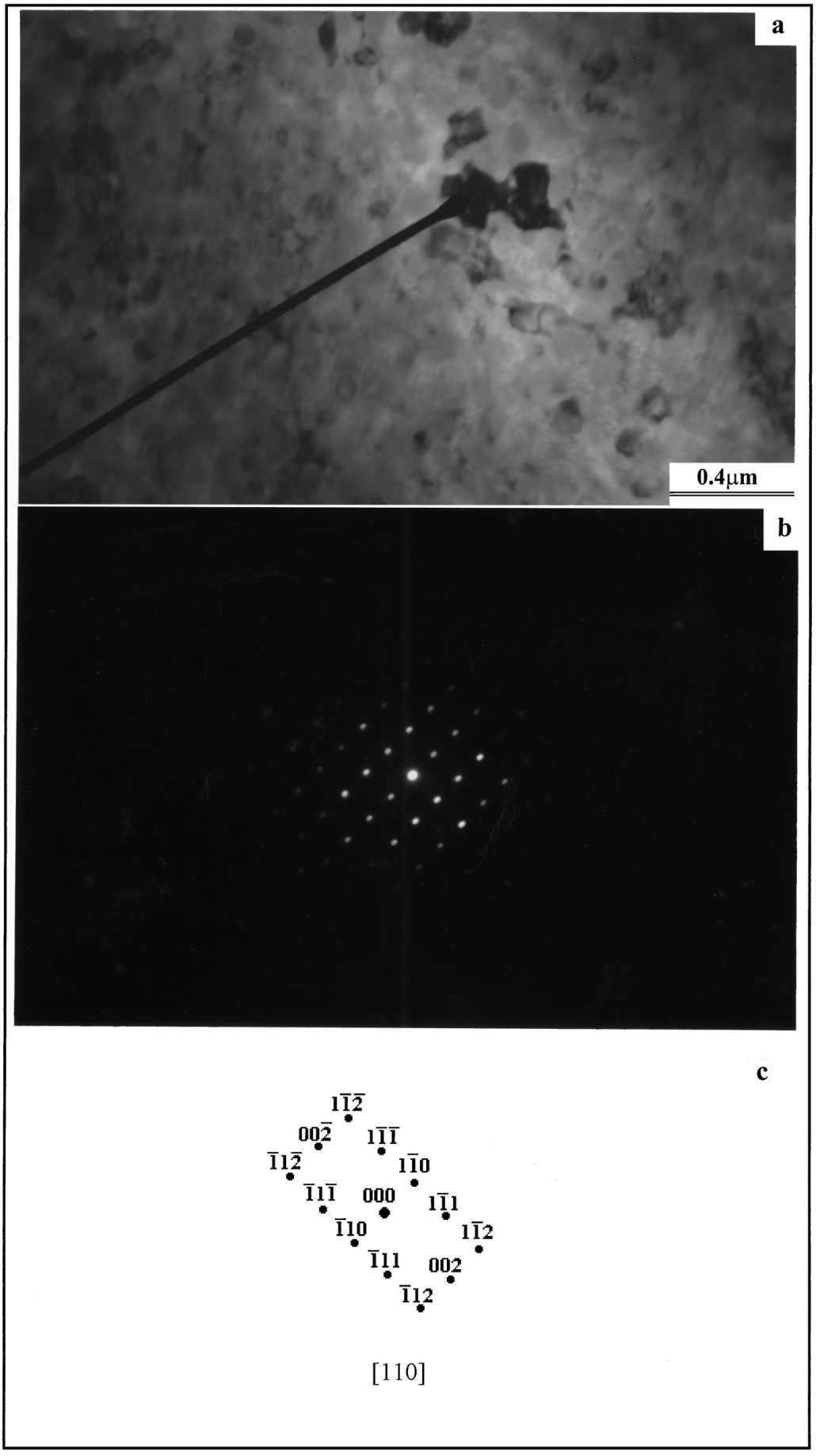

Figure 5 (a) BF TEM image, (b) corresponding SADP solved in (c); a crystalline region (indicated by pointer) observed in G5P-glass heated 93 h at 800 °C. The SADP was indexed as [110] for stable LS_2.

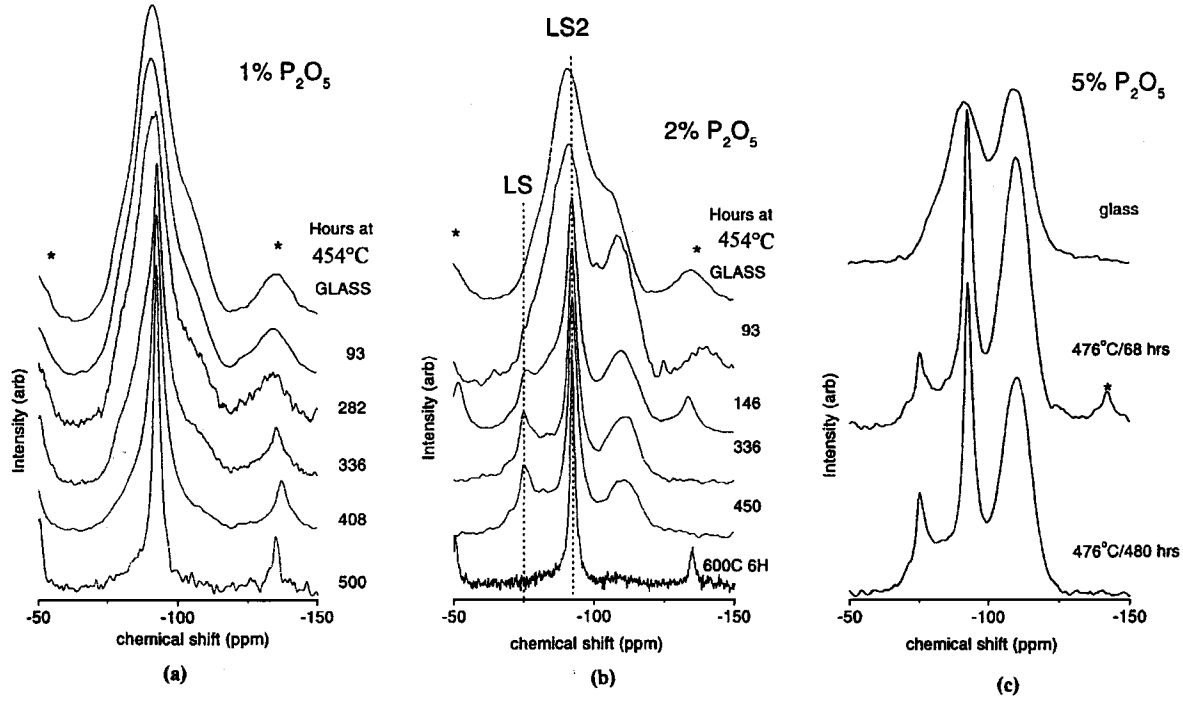

Figure 6 ^{29}Si MAS-NMR spectra of (a) G1PF: as-quenched glass and heated at 454 °C for times (hours) indicated, (b) G2PF: as-quenched glass and heated at 454 °C for times (hours) indicated and at 600 °C for 6 h and (c) G5PF: as-quenched glass and heated at 476 °C for 68 and 480 h.

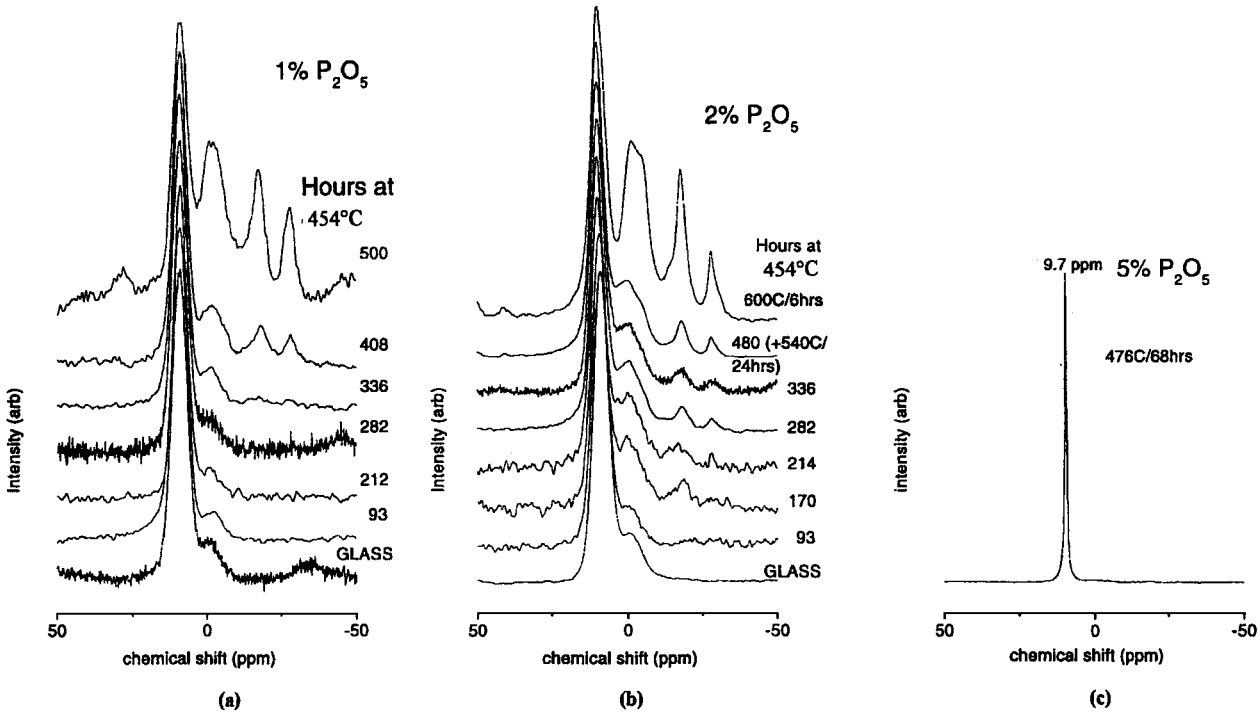

Figure 7 ^{31}P MAS-NMR spectra of (a) G1PF, (b) G2PF and (c) G5PF. G1PF and G2PF traces for as-quenched glasses and glasses heated at 454 °C for times (hours) indicated. G5PF (c) heated for 68 h at 476 °C.

trends were observed for each P_2O_5-concentration but with changes occurring at progressively shorter times as the concentration of P_2O_5 increases. This is illustrated in Fig. 10 where the amount of LS_2 formed is plotted against time at temperature for glasses with 0, 2 and 5 mol % P_2O_5. It can be seen that the induction period for crystal growth decreases with P_2O_5 content (0 and 2 mol % P_2O_5 glasses heated at 454 °C) and is effectively absent in the 5 mol % P_2O_5 samples (heated at 476 °C).

4. Discussion

XRD of the phosphate containing compositions G1P and G2P after heat treatments at 454 and 476 °C revealed volume crystallisation of the same metastable phases α'- and β'-LS_2 previously found in the early stages of crystallisation of the binary lithium disilicate (LS_2) glass after extended heat treatments at 454 °C (the LS_2 glass was denoted by G1 in the previous paper [25]). The XRD observations in G1P and G2P were similar to those in G1 except that the phases appeared

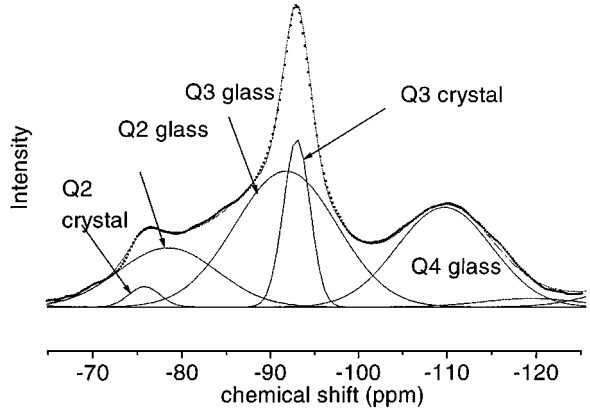

Figure 8 Example of the fitting of a typical ^{29}Si spectrum (G2PF heated 146 h at 454 °C). Only the isotropic peaks are shown here but fitting is also applied to the spinning sidebands to obtain the relative amounts of each species (after [31]).

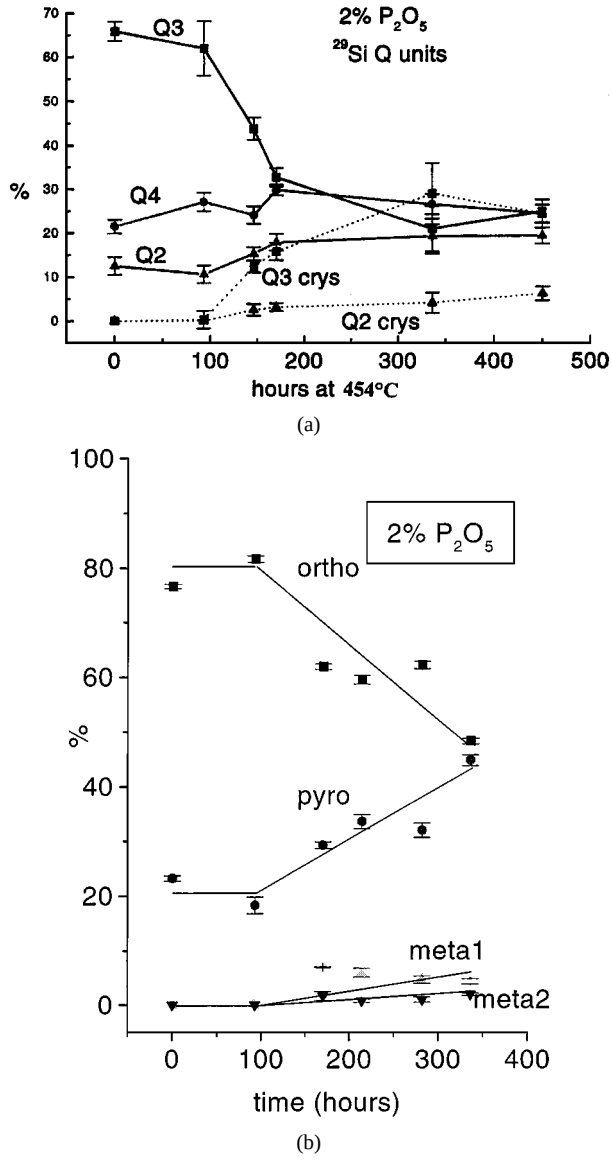

Figure 9 Variation of the relative amounts of different (a) Q species and (b) phosphate units in G2PF with time at 454 °C. Lines are drawn to guide the eye (after [31]).

after different times. This can be attributed to a combination of two effects of P_2O_5 addition, namely an increase in viscosity (as observed by Matusita and Tashiro [4]) and a possible alteration in nucleation rates of the metastable phases (an increase in nucleation rate of the stable LS_2 phase was observed in previous work [2]). Evidence of metastable phase formation (including possible lithium metasilicate formation) was also found in the G5P (5 mol % P_2O_5 addition) glass.

As in the previous study [25] the presence of the metastable phases observed by XRD could not be confirmed by selected area diffraction in the TEM (although fine crystals were observed by TEM) because of the extreme sensitivity of these phases to the electron beam. Only the equilibrium lithium disilicate phase was identified after long heat treatments at 454 °C and above. It has not been possible, therefore, to elucidate the influence of the metastable phases on the crystallisation of the equilibrium LS_2 in these phosphate containing glasses or in G1 [25]. There is so far no direct evidence for heterogeneous nucleation of stable LS_2 on the metastable phases, or that the latter definitely transform with time to stable LS_2. Since these precursor phases have only been observed for extremely long heat treatments at temperatures near the glass transformation temperature they may have little or no influence on the later stage nucleation and crystallisation processes including the appearance of stable LS_2 at higher temperatures. Further experimental work may resolve these questions.

Optical microscopy studies of the LS_2 glass (G1) and G1P clearly showed that addition of P_2O_5 caused an increase in the number of stable LS_2 crystals for heat treatment at 476 °C, i.e. an increase in the nucleation rate of this phase, in agreement with previous work [2]. Also from the difference in average crystal sizes, the crystal growth rate at 476 °C in G1P was smaller than in G1, indicating a larger viscosity in G1P, again in agreement with previous studies [4, 11].

The apparent morphology of crystals observed by TEM in G1P after 190 h at 463 °C was approximately ellipsoid-shaped and the ratio of dimensions along the *a* and *b* axes was about 2 : 1, which is smaller than the 4 : 1 observed in G1 after 120 h at 454 °C [25], indicating that addition of P_2O_5 changed the crystal morphology. A schematic diagram of these morphologies is shown in Fig. 11. Lithium disilicate has a layer type structure [28] in which the corrugated sheets of Si_2O_5 composition parallel to (010) are linked by Li^+. Consequently the bonding between layers is expected to be weaker than the bonding within layers. This gives rise to a marked anisotropy in surface energy as a function of crystallographic orientation and therefore a higher $a : b$ ratio in the binary LS_2 glass [29, 30]. The decrease in ratio on adding P_2O_5 indicates that the crystal/liquid interfacial energy has been altered as a function of crystallographic orientation and has become more isotropic, but it is not possible to say if the average value has decreased or increased.

An important result of the present work was the observation from XRD of the presence of Li_3PO_4 in the as-quenched G5P glass, indicating that Li_3PO_4 was precipitated on cooling in this glass. Heat treatment at 476 °C led to further crystallisation of Li_3PO_4, and formation of metastable α'-LS_2, prior to formation of stable LS_2. This observation suggests that Li_3PO_4 crystals may be acting as heterogeneous nucleation sites for stable

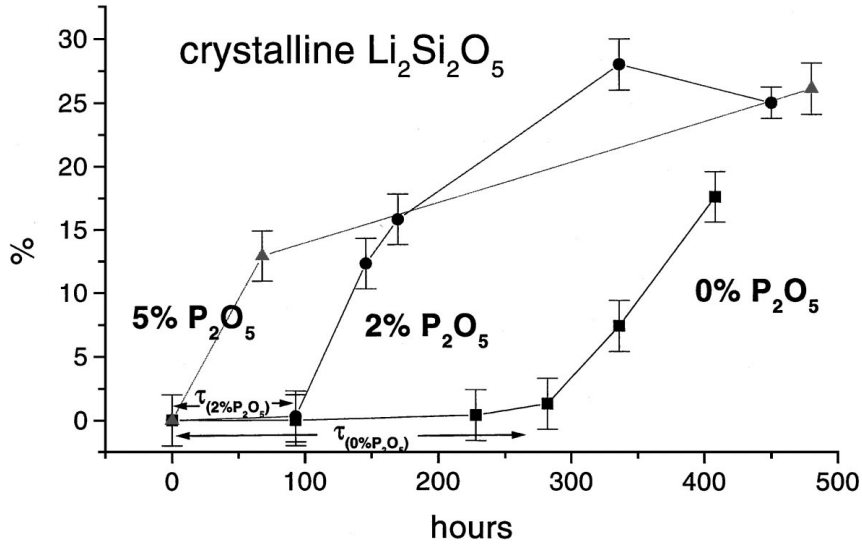

Figure 10 Percentage of silicon present as crystalline LS_2 as a function of heat treatment time for glasses of different P_2O_5 contents. G1F and G2PF glasses were heat treated at 454 °C and G5PF glass heat treated at 476 °C. Approximate induction times (τ) to onset of crystallisation are indicated for G1F and G2PF.

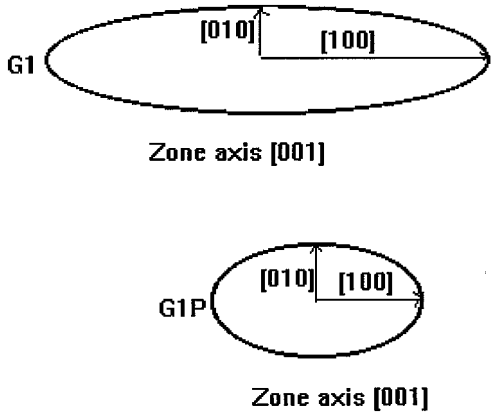

Figure 11 Schematic of the observed crystal morphologies in G1 and G1P, showing slower growth along [100] due to 1 mol % P_2O_5 addition.

LS_2 and would explain the enhanced nucleation rates observed on addition of P_2O_5. Although no Li_3PO_4 or phosphate containing phase, was detected in G1P and G2P prior to LS_2 crystallisation, this may be accounted for by the volume fraction of these phases being too low to be detected by XRD in G1P and G2P, which only contained 1 and 2 mol % P_2O_5 respectively.

However, no Li_3PO_4 crystals could be observed by TEM in G1P, G2P and G5P. As mentioned previously, fine crystalline particles (<0.1 μm) possibly of the metastable α'-LS_2 phase were detected by TEM but identification was impossible due to their rapid decomposition. A similar explanation may apply for the non-observation by TEM of Li_3PO_4, although detected by XRD in G5P glass. These tiny particles may be associated with the Li-P units detected by MAS-NMR.

As revealed by MAS-NMR, the relative proportion of the Q^3-X does not appear to agree with that expected from the XRD study and the species were detected significantly later than that by XRD. Two possible reasons for this are (a) the glasses were prepared as different batches with that for NMR having 0.05 mol % Fe_2O_3 added-thus there may be small compositional and thermal history differences between the two sets of glasses; (b) the Q^3-X peak formed after long times at 454 °C is noticeably broader than that from the phase formed at 600 °C although the XRD pattern is identical. This implies that the ^{29}Si in the 454 °C LS_2 phase has a range of very similar environments which become identical at higher temperature. It is possible that the metastable LS_2 phase observed in the earlier stages by XRD contains a range of ^{29}Si environments which is even wider and the resulting resonance is both broad and coincident with the amorphous Q^3 peak and therefore difficult to detect.

In addition to the change in the intensities of some of the Q^n resonances, there is also a progressive shift in the position of the Q^4 peak from that expected for Q^4 surrounded by Q^3 to that for Q^4 surrounded by Q^4 (Fig. 6). This indicates that glass-in-glass phase separation is occurring to produce a droplet phase which is largely amorphous silica. This is further supported by the change in the relaxation time of the Q^4 resonance. This increases with increasing time at 454 °C and indicates that the Fe^{3+}, included in the composition to decrease the relaxation time of ^{29}Si, is segregating from the droplet silica phase into the lithium silicate matrix. In fact it is extremely likely that amorphous phase separation was present after heat treatment of G1P, G2P and G5P based on similar compositions in previous work [2, 4, 7, 11]. The reasons for failure to observe phase separation by TEM in the present work is probably the extremely fine size of the droplets for the relatively low heat treatment temperatures used and the poor contrast of the droplets in the ion beam thinned specimens compared to the chemically thinned (etched) samples used by James and McMillan [8].

As stated in Section 3.3, the phosphate units formed are associated with some of the Li^+ ions in the glass to give orthophosphate (Li_3PO_4) units at 9.7 ± 0.3 ppm and pyrophosphate ($Li_4P_2O_7$) units at 0.0 ± 0.2 ppm. As time at temperature (454 °C) is increased, there is a change in the relative proportions of the two units and also the formation of two types of metaphosphate units with different chain lengths, at -17.9 ± 0.2 ppm and -28.3 ± 0.2 ppm (Fig. 9b). At this temperature there is

no evidence of crystalline Li_3PO_4, the phase which has been suggested to form heterogeneous nucleation sites for stable LS_2, in the 1 or 2 mol % P_2O_5 materials but there is crystalline Li_3PO_4 in the 5 mol % P_2O_5 glass, i.e. it is formed on cooling of the melt in agreement with XRD (Fig. 2a). There is some crystalline phosphate at 600 °C but it is the metaphosphate crystal which forms. The start of the change in the population of phosphate species corresponds to the time when crystallisation of the silicate network becomes apparent. The formation of LS_2 depletes the glass phase of Li^+ which is then replenished by removal from the phosphate ions and leads to their repolymerisation, giving extra pyrophosphate and metaphosphate.

5. Summary and conclusions

(1) XRD of lithium disilicate glasses containing $\leq$2 mol % P_2O_5 heated at 454 °C for various times indicated formation of metastable α'- and β'-LS_2 phases at early and intermediate stages of crystallisation and their probable transformation to stable LS_2 at later stages. Since peaks due to silicate phases appeared after shorter times in samples with higher P_2O_5 concentration (>1 mol %), β'-LS_2 peaks could not be seen in G5P. In addition, due to the higher P_2O_5 concentration in G5P, the Li_3PO_4 crystal phase was detected by XRD in the as-quenched as well as in heat treated samples.

(2) Addition of P_2O_5 caused an increase in the nucleation rate of the stable lithium disilicate phase, and a decrease in the crystal growth rate, for heat treatments at 476 °C, supporting previous studies.

(3) Addition of P_2O_5 altered the morphology of stable LS_2 crystals observed by TEM at later stages of heat treatment indicating a change in the crystal/liquid interfacial energies with crystallographic orientation.

(4) Electron beam damage of nucleated samples precluded the identification of metastable phases by TEM at the earliest stages of crystallisation, and prevented observation of Li_3PO_4 crystals by TEM at the later stages.

(5) Apart from Q^3 which was the major species observed, ^{29}Si MAS-NMR indicated the presence of significant amounts of Q^2 and Q^4 in as-quenched and heat treated glasses. The chemical shift and T values for Q^4 indicated phase separation in the G2PF glass which could not be detected with XRD/TEM. ^{31}P MAS-NMR showed the presence of amorphous lithium orthophosphate along with pyro- and meta-phosphate units. At 454 °C heat treatments there was no evidence of crystalline Li_3PO_4 in the 1 or 2 mol % glasses but there was crystalline Li_3PO_4 in the 5 mol % P_2O_5-glass, in agreement with the XRD.

(6) The observation of crystalline Li_3PO_4 in the 5 mol % P_2O_5 glass provides supporting evidence for the suggestion that Li_3PO_4 crystals act as sites for heterogeneous nucleation of stable LS_2 crystals [8, 9, 11, 13] at the relatively low temperatures around the transformation range used in the present work. However, it was not possible to detect Li_3PO_4 in the 1 and 2 mol % P_2O_5 glasses possibly because of the small volume fractions of Li_3PO_4 involved. Thus the question of heterogeneous nucleation was not conclusively resolved.

Acknowledgement

We wish to thank Elsevier Science for permission to reproduce figures 3(b), 5 and 6(b) from Holland *et al*. Journal of non-crystalline solids **232–234** (1998) 140 (see Ref. [31] below).

References

1. P. F. JAMES, *Phys. Chem. Glasses* **15**(4) (1974) 95.
2. P. F. JAMES, "Adv. in Ceramics," Vol. 4, edited by J. H. Simmons, D. R. Uhlmann and G. H. Beal (Amer. Ceram. Soc., Columbus, Ohio, 1982) p. 1.
3. P. F. JAMES, "Glasses and Glass Ceramics" (Chapman and Hall, 1989, 59).
4. K. MATUSITA and M. TASHIRO, *Phys. Chem. Glasses* **14**(4) (1973) 77.
5. W. VOGEL, "Structure and Crystallisation of Glasses" (Pergamon Press, New York, 1971) 82.
6. T. I. BARRY, in Phase Transformations, Spring Residential Conf. Series 3, **1** (1979) 1201-79-Y, pp. III-1, Published by Institution of Metallurgists (Chameleon Press).
7. S. V. PHILLIPS and P. W. MCMILLAN, *Glass Technology* **6**(2) (1965) 46.
8. P. F. JAMES and P. W. MCMILLAN, *Phys. Chem. Glasses* **11**(3) (1970) 59.
9. *Idem., J. Mater. Science* **6** (1971) 1345.
10. R. H. DOREMUS and A. M. TURKALO, *Phys. Chem. Glasses* **13**(1) (1972) 14.
11. H. HARPER and P. W. MCMILLAN, *ibid.* **13**(4) (1972) 97.
12. M. TOMOZAWA, *ibid.* **13**(6) (1972) 161.
13. T. J. HEADLEY and R. E. LOEHMANN, *J. Amer. Ceram. Soc.* **67** (1984) 620.
14. A. M. KALININA, V. M. FOKIN, G. A. SYCHEVA and V. N. FILIPOVICH, in Proceedings of the XIV Intl. Cong. on Glass, New Delhi, India (Indian Ceram. Soc., 1986) p. 366.
15. P. F. JAMES, Unpublished data, University of Sheffield, 1980.
16. P. W. MCMILLAN, Tenth Inter. Cong. on Glass, Part II, 1974 pp. 14-1.
17. R. DUPREE, D. HOLLAND and M. G. MORTUZA, *Phys. Chem. Glasses* **29**(1) (1988) 18.
18. A. R. GRIMMER, M. MAGI, M. HAHNERT, H. STADE, A. SAMOSON, W. WIEKER and E. LIPPMAA, *ibid.* **25**(4) (1984) 105.
19. R. DUPREE, D. HOLLAND and M. G. MORTUZA, *J. Non-Cryst. Solids* **116** (1990) 148.
20. J. W. ADAMS, "Morphogenesis in Lithium Disilicate Glass: Internal Nucleation in Amorphous Structures," PhD thesis, University of Cambridge, 1993.
21. R. J. KIRKPATRICK, *Reviews in Mineralogy* **18** (1988) 341.
22. R. DUPREE and D. HOLLAND, in "Glasses and Glass Ceramics," edited by M. H. Lewis (Chapman & Hall, London, 1989) p. 1.
23. J. F. EMERSON, P. E. STALLWORTH and P. J. BRAY, *J. Non-Cryst. Solids* **113** (1989) 253.
24. J. F. STEBBINS, P. F. MCMILLAN and D. B. DINGWELL, in *Reviews in Mineralogy* **32** (1995) 191.
25. Y. IQBAL, W. E. LEE, P. F. JAMES and D. HOLLAND, *J. Non-Cryst. Solids* **224** (1998) 1.
26. M. AL-KHAFAJI, Personal Communication, Sorby Centre for Electron Microscopy, University of Sheffield, 1995.
27. J. P. MORNIROLI, L. WINTER and D. VANKIEKEN, Electron Diffraction Computer Program, "DIFFRACT," vers. 3.4, 1995.
28. V. F. LEIBAU, *Acta Cryst.* **14** (1961) 389.
29. E. G. ROWLANDS and P. F. JAMES, *Phys. Chem. Glasses* **20**(1) (1979) 9.
30. P. F. JAMES and S. R. KEOWN, *Phil. Mag.* **30** (1974) 789.
31. D. HOLLAND, Y. IQBAL, P. F. JAMES and W. E. LEE, *J. Non-Cryst. Solids* **232–234** (1998) 140.

Received 11 November 1998
and accepted 15 March 1999